# Effects of defect density and back contacts on the performance of $Cu_2O/TiO_2$ thin film solar cell

A. K. BISWAS[1*], S. BISWAS[2], S. S. BISWAS[3]
[1]*Department of Physics, NabadwipVidyasagar College, Nabadwip, Nadia-741302, West Bengal, India*
[2]*Department of Physics, Fulia Sikshaniketan Govt. Sponsored School, Santipur, Nadia, West Bengal, India*
[3]*Department of Physics, Surendranath College, 24/2, M. G. Road, Kolkata-700009, West Bengal, India*

Defects in various layers of solar cells play an important role in determining the characteristics of such devices. Different types of defects such as acceptor type in $Cu_2O$ layer, donor type in $TiO_2$ layer and neutral type on the interface ($Cu_2O/TiO_2$) have been considered to simulate the proposed solar cell with the help of SCAPS-1D software. Results obtained from this simulation show that output parameters like short circuit current density ($J_{SC}$), open circuit voltage ($V_{OC}$), fill factor (FF) and power conversion efficiency (PCE) significantly depend on the defect density and its properties. Appropriate selection of defect density of corresponding layers may improve the device performance. Moreover, different back contact metals (Cu, Ag, Fe, Nb, Mo, Ni, Au, Pt) have been taken step by step during simulation for understanding the effects of such back contacts. It is observed that solar cell gives better results when Ni (5.22 eV) acts as back contact.

(Received April 10, 2025; accepted February 2, 2026)

*Keywords:* Defect density, Interface, Work function, Solar cell, Heterojunction

## 1. Introduction

Global energy demand is growing tremendously due to factors like increased population, rapid industrialisation, and the widespread use of digital technologies in almost every part of our daily lives. Fossil fuels serve as the primary source of energy, but they are not a renewable source of energy [1-2]. In this situation, solar cells have great potential to replace fossil fuels as a cleaner and more sustainable energy source. In the early days, solar cells were produced using silicon. But, the production of silicon-based solar cells is more complex and expensive than metal oxide semiconductor-based thin film solar cells. Hence, many researchers have focused their attention on semiconducting metal oxide for designing and fabricating thin film solar cells in the last few years [3-7]. In these studies, various semiconducting oxides have been used in thin film solar cells by different techniques and investigated correspondingly to improve the device performance. Metal oxide semiconductors (MOs) have emerged as promising materials for optoelectronics and photovoltaic applications because of their non-toxic and chemically stable characters [8-10]. These materials have been used extensively in thin film solar cells due to their low production costs and easy utilising techniques compared to traditional silicon-based solar cells [11-13]. There are many reports on solar cells available in the literature in which copper oxide is used as an active layer [14-16]. Conversion efficiency of a solar cell is the most significant parameter, which has theoretically reached 20% for a $Cu_2O$ based solar cell [16], but the experimentally highest obtainable conversion efficiency is 3.83% for $Cu_2O$ substrate [17]. Various attempts have been made by researchers on copper oxide, zinc oxide and titanium oxide solar cells using different fabricating techniques to enhance the efficiency of corresponding devices [17-21]. Several works have been done on various types of solar cells, considering the effects of different types of defects present in cell layers and also the role of layer thickness in improving the cell performance [22-27]. Along with defect density, back contact metals have adverse effects on solar cell performance. Influences of different back contacts on the solar cell's characteristics have been extensively studied [28-32]. Since very little work has been done on $Cu_2O/TiO_2$ thin film solar cells considering the effects of defect density and back contacts, authors have made the decision to carry out their research on the proposed solar cell taking the effects of defect density and different back contacts on the output parameters of the selected device for further investigation.

## 2. Material properties and model details

Structure of the proposed $Cu_2O/TiO_2$ solar cell and corresponding energy band diagram have been shown in Fig. 1 and Fig. 2, respectively. Cuprous oxide ($Cu_2O$) is a well known stable oxide of copper, and it is a naturally formed p-type semiconductor [33]. Optical and electrical properties of this material have been reported in the literature [34, 35]. First, cuprous oxide ($Cu_2O$) was used for photovoltaic applications in 1978 by the National Science Foundation and Joint Centre [36, 37]. Cuprous oxide carries low electron affinity (3.2 eV) [36, 38, 39] and very high hole mobility [36, 40]. This character makes $Cu_2O$ a hole transport material in heterojunction solar cells [36, 41]. A few applications of $Cu_2O$ as n-type semiconductors have been found in the literature and the reported efficiencies are very low [42]. On the other hand, Titanium dioxide ($TiO_2$) is a transition metal oxide. Its favourable optical and electronic properties have attracted researchers to study this material for making solar cells in the last decade [43]. Besides, $TiO_2$ is a durable and high refractive material that can be a necessary component for electronic devices [44]. Front contact of the solar cell is FTO (fluorine doped tin oxide), a highly transparent conducting material whose work function is 4.4 eV [45]. The work function of the back contact metal (Ni) is chosen 5.22 eV [30].

Several numerical simulation tools like AFORS-HET [46], AMPS [47], ASPIN [48] and SCAPS [49] are available for characterising especially thin film heterojunction junction solar cells [50]. Among these tools SCAPS-1D has been taken here to simulate the proposed $Cu_2O/TiO_2$ thin film solar cell under different conditions. SCAPS-1D is windows-based application software, developed by Marc Burgelman and his Associates at the University of Gent, Belgium [49, 51]. User can set the required parameters of materials used in the solar cell as well as operating temperature, voltage, frequency and illumination [49-52] to calculate the results in the form I-V, C-V, C-f, Q(λ), band diagram, electric field, carrier densities, partial recombination currents etc. SCAPS software initially solves Poisson's equation along with the continuity equations for electrons and holes to perform such operations. This software can permit a solar cell composed of up to a maximum seven semiconductor layers with specified properties, separate entries for interface parameters and two additional layers for front and back contacts [52]. Authors have carried out their simulation-based work with the help of software package SCAPS-1D version 3.3.10 [52], taking the physical parameters mentioned in Tables 1, 2, 3 and under one sun AM 1.5 G spectrum.

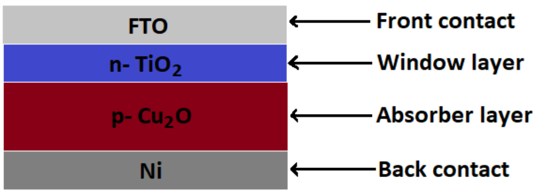


*Fig. 1. Structure of the proposed solar cell (colour online)*

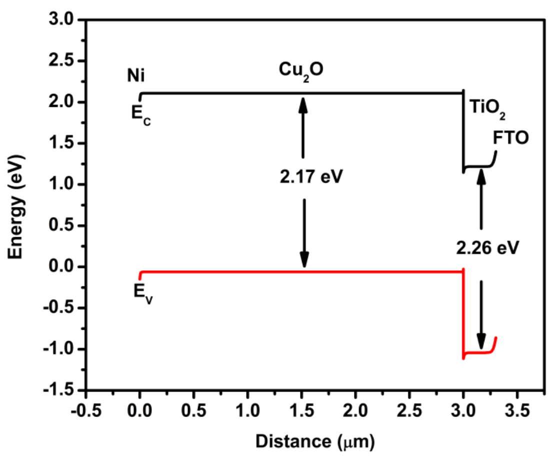


*Fig. 2. Energy band diagram of the cell (colour online)*

*Table 1. Input properties of $TiO_2$ and $Cu_2O$ [23, 34-36]*

| Properties | n- $TiO_2$ | p- $Cu_2O$ |
|---|---|---|
| Band gap (eV) | 2.26 | 2.17 |
| Electron affinity (eV) | 4.20 | 3.20 |
| Relative dielectric permittivity | 10.0 | 7.11 |
| Effective density of states in CB ($cm^{-3}$) | $2.0\times10^{17}$ | $2.0\times10^{17}$ |
| Effective density of states in VB ($cm^{-3}$) | $6.0\times10^{17}$ | $1.1\times10^{19}$ |
| Electron mobility($cm^2$/Vs) | 100 | 200 |
| Hole mobility($cm^2$/Vs) | 25 | 80 |
| Shallow uniform donor density ($cm^{-3}$) | $1.0\times10^{17}$ | 0 |
| Shallow uniform acceptor density ($cm^{-3}$) | 0 | $1.0\times10^{18}$ |

*Table 2. Defect parameters of $TiO_2$, $Cu_2O$ and interface [24, 27]*

| Properties | n- $TiO_2$ | p- $Cu_2O$ | Interface ($Cu_2O/TiO_2$) |
|---|---|---|---|
| Defect type | Donor (+/0) | Acceptor (-/0) | Neutral |
| Capture cross section electrons ($cm^2$) | $1\times10^{-13}$ | $1\times10^{-15}$ | $1\times10^{-19}$ |
| Capture cross section holes ($cm^2$) | $1\times10^{-15}$ | $1\times10^{-13}$ | $1\times10^{-19}$ |
| Energetic distribution | Single | Single | Single |
| Reference for defect energy level Et | Above $E_V$ | Above $E_V$ | Above highest $E_V$ |
| Energy level with respect to reference (eV) | 1.2 | 0.55 | 1.0 |
| Uniform defect density | $10^{12}-10^{18}\ cm^{-3}$ | | $10^{10}-10^{15}\ cm^{-2}$ |

*Table 3. Contact parameters [30, 45]*

| Parameter | Left contact | Right contact |
|---|---|---|
| Surface recombination velocity of electrons (cm/s) | $1\times10^{0}$ | $1\times10^{7}$ |
| Surface recombination velocity of holes (cm/s) | $1\times10^{7}$ | $1\times10^{0}$ |
| Metal work function (eV) | Ni (5.22), and varied | 4.4 |
| Majority carrier barrier height relative to $E_F$ (eV) | 0.15 | 0.2 |
| Majority carrier barrier height relative to $E_V$ or $E_C$ (eV) | 0.0879 | 0.182 |

## 3. Results and discussion

The SCAPS-1D Program offers several types of defects which may be selected for modelling solar cells. In this study, acceptor, donor and neutral defects were considered, respectively, in the absorber layer, window layer and on the interface. Different types of defects affect the carrier lifetime and diffusion length according to the relations $\tau = 1/\sigma N_t V_{th}$ and $L = \sqrt{D\tau}$, where the symbols have their usual meanings [52]. Besides, different back contacts have also been considered here for analysis. The Schottky barrier builds up if $\phi_m < E_g + (\delta_{Abs} + \phi_d)$, where $\phi_m$ is the work function of the back contact metal, $E_g$ is the band gap, $\delta_{Abs}$ is the electron affinity of the absorber material, $\phi_d$ is the difference in energy between the valence (or conduction) band in bulk and at the edge. The Schottky barrier ($\phi_s$) at the metal contact is given by the equation $\phi_s = \phi_m - E_V$, where $E_V$ is the valence band energy. For a particular absorber material, Schottky barrier height can be controlled by selecting a back contact of work function close to $(E_g + \phi_d + \delta_{Abs})$ [53].

### 3.1. Impact of defects in absorber ($Cu_2O$) and window ($TiO_2$) layers

Defects in a solar cell significantly influence its performance, after affecting its efficiency, carrier lifetime, and overall energy conversion. Acceptor or Donor type defects typically refer to the introduction of additional energy states within the band gap of the semiconductor material, which can alter charge carrier dynamics and consequently, the overall efficiency of the solar cell. The defect densities of the absorber and window layers are varied separately from $10^{12}$ cm$^{-3}$ to $10^{18}$ cm$^{-3}$, keeping the defect density of the window layer (or absorber layer) $10^{14}$ cm$^{-3}$ and the defect density of interface $10^{11}$ cm$^{-2}$, and all other parameters the same to examine the output characteristics of solar cell. Simulation results are shown in Fig. 3, Fig. 4, Fig. 5 and Fig. 6 respectively as a function of defect density. It is observed that short circuit current density ($J_{SC}$), open circuit voltage ($V_{OC}$), fill factor (FF) and power conversion efficiency (PCE) remain constant up to the defect density of $10^{14}$ cm$^{-3}$ and after this value, device parameters reduce gradually. It can be explained that an increase in defect density indicates more and more traps, which promote recombination of excess minority carriers and reduce carriers' lifetime according to Shockley-Red hall theory. It may be mentioned that solar cell parameters are more affected by enhancing defect density of the window layer than that of the absorber layer [23, 54-55].

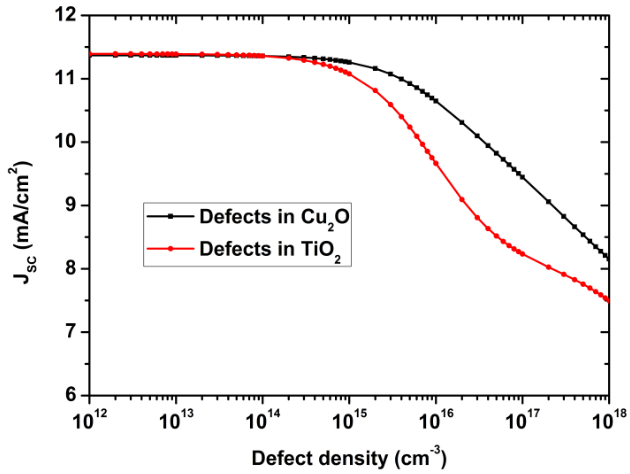


*Fig. 3. Short circuit current with defect density (colour online)*

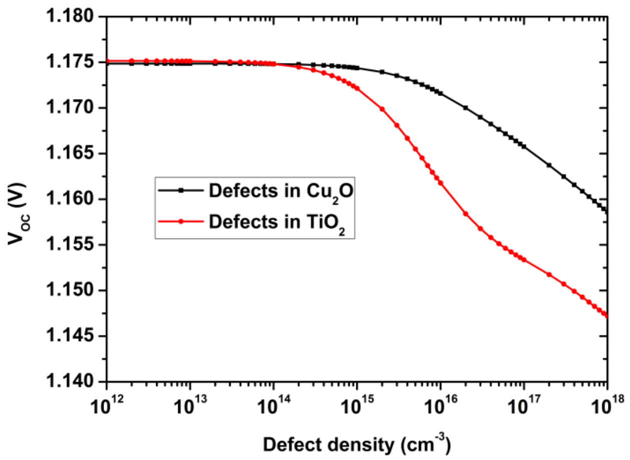


*Fig. 4. Open circuit voltage with defect density (colour online)*

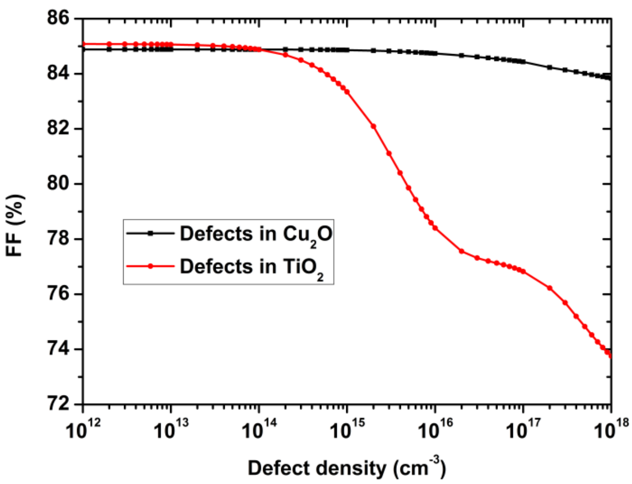


*Fig. 5. Fill factor with defect density (colour online)*

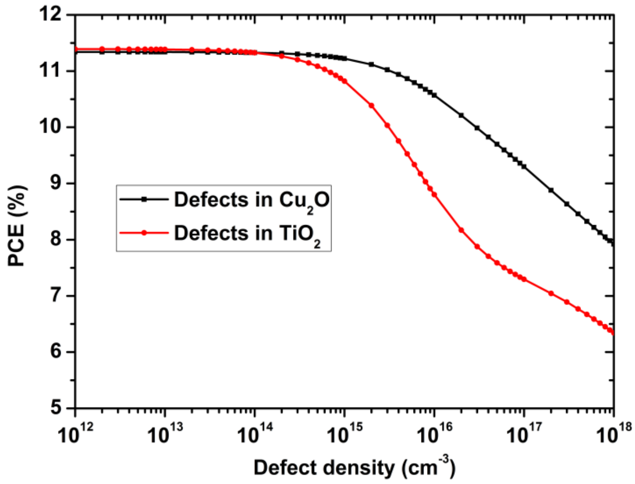


*Fig. 6. Power conversion efficiency with defect density (colour online)*

### 3.2. Impact of interface defect

The presence of interface neutral defects between the window and absorber layers in solar cells can impact the device's efficiency in various ways. Since neutral defects are neither positively nor negatively charged, their effects are more complex and often depend on the nature of the interface and the materials used in the solar cell. Neutral defects at the interface can act as recombination centres for charge carriers (electrons and holes) that are generated by light absorption. When charge carriers reach the interface, they are trapped by these neutral defects, where they recombine before contributing to the external current. The increased recombination reduces the open-circuit voltage ($V_{OC}$) and short-circuit current ($J_{SC}$), both of which are crucial for controlling the overall efficiency of the solar cell. Higher recombination rates at the interface can significantly lower the power conversion efficiency (PCE) of the device. In this computer simulation, interface defect density is controlled from $10^{10}$ $cm^{-2}$ to $10^{15}$ $cm^{-2}$, keeping other parameters fixed. Results obtained from this simulation are shown graphically in Fig. 7, Fig. 8, Fig. 9 and Fig. 10 for different values of interface defect density. Observed results indicate that solar cell parameters begin to deteriorate as the defect density of the interface increases gradually after $10^{13}$ $cm^{-2}$. More and more neutral defects of the interface bring more and more recombination traps where charge carriers are lost by recombination. This reduces carrier lifetime as well as carrier diffusion length, which results in lower device performance. Similar results have been obtained and discussed by other researchers [23].

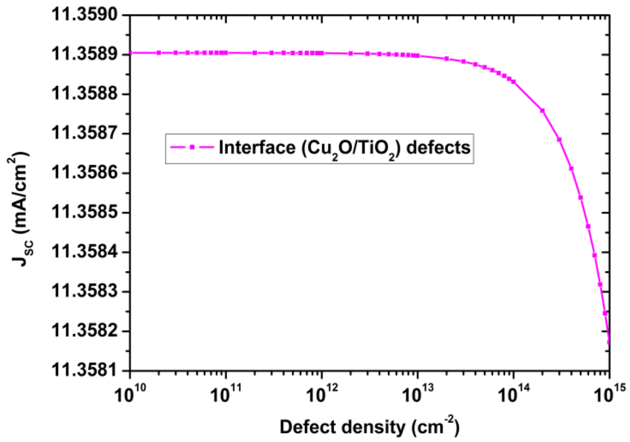


*Fig. 7. Short circuit current density with defect density of interface (colour online)*

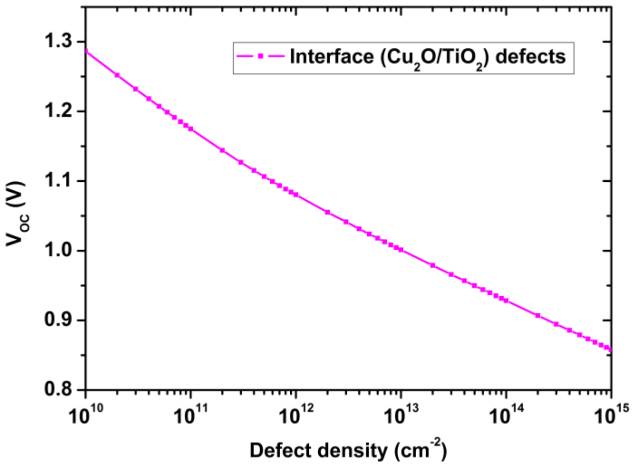


*Fig. 8. Open circuit voltage with defect density of interface (colour online)*

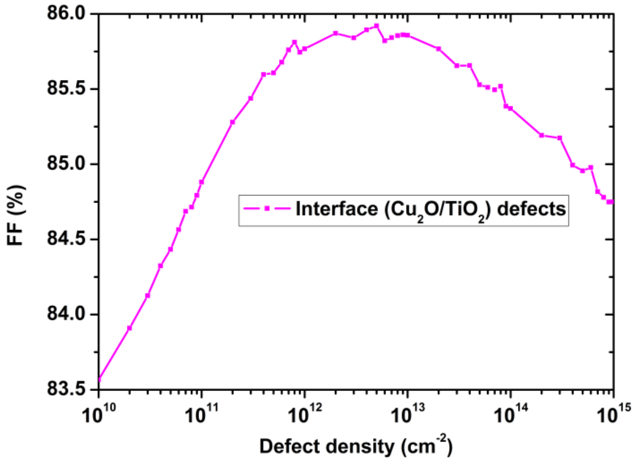


*Fig. 9. Fill factor with defect density of interface (colour online)*

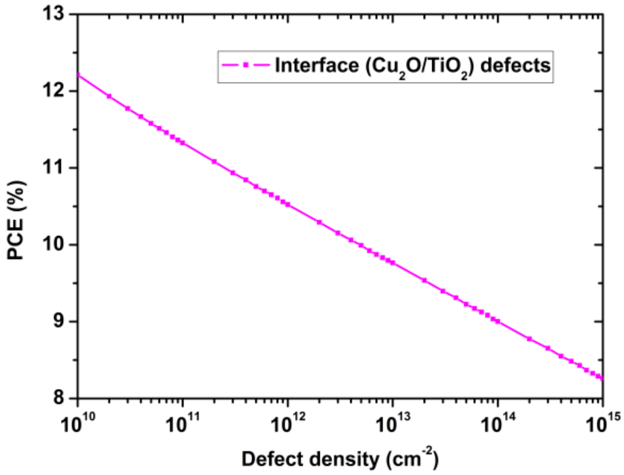


*Fig. 10. Power conversion efficiency with defect density of interface (colour online)*

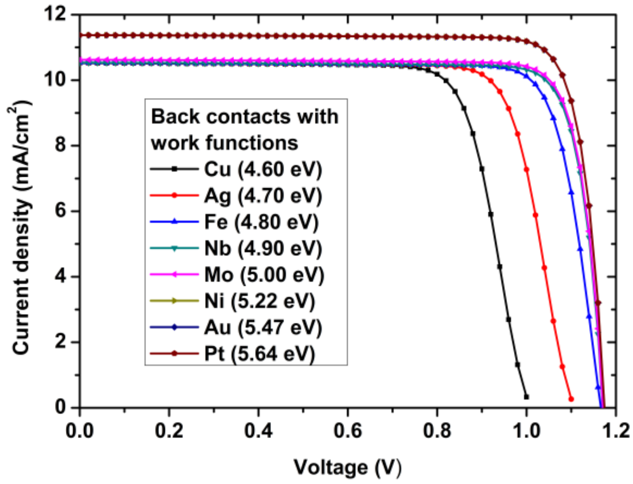


*Fig. 11. Current density versus voltage for different back contact metals (colour online)*

### 3.3. Role of back contacts

The back contact metal plays a critical role in measuring the performance of solar cells. It serves as the interface between the semiconductor and the external circuit, facilitating the extraction of the photogenerated charge carriers (electrons or holes) from the solar cell. The properties of the back contact metal, including its work function, conductivity, stability, and adhesion, can significantly impact the overall efficiency, voltage, current, and stability of the solar cell. The contact resistance between the semiconductor and the back contact metal is another critical factor. This resistance can be affected by the choice of back contact metal, its work function and the quality of the interface between the metal and the semiconductor. High contact resistance reduces the fill factor (FF), open circuit voltage ($V_{OC}$) and hence overall efficiency of the solar cell. If the work function of the back contact metal is too high or too low compared to the semiconductor, it creates a schottky barrier that limits efficient carrier extraction. Here, the work function property of the back contact has been considered for analysis. Different back contact metals with their work functions have been taken separately during simulation to get better results. The defect densities of the absorber, window layers and interface were set at $10^{14}$ cm$^{-3}$ and $10^{11}$ cm$^{-2}$, respectively, and the values of other parameters were selected as per Tables 1, 2, 3 while simulation. Current – voltage characteristics for various back contacts are highlighted graphically in Fig. 11, and also numerical results are mentioned in Table 4. It is observed from these results that solar cell gives higher short circuit current density and open circuit voltage as the work function of back contact metals reaches 5.22 eV. Similar studies on other solar cells have been performed by researchers previously [30, 53].

*Table 4. Solar cell parameters for different back contacts*

| Back contacts | $V_{OC}$ (V) | $J_{SC}$ (mA/cm$^2$) | FF (%) | PCE (%) |
|---|---|---|---|---|
| Cu | 1.0065 | 10.502 | 77.20 | 8.16 |
| Ag | 1.1051 | 10.509 | 82.25 | 9.08 |
| Fe | 1.1660 | 10.515 | 82.25 | 10.08 |
| Nb | 1.1710 | 10.520 | 84.64 | 10.43 |
| Mo | 1.1714 | 10.606 | 84.76 | 10.57 |
| Ni | 1.1748 | 11.358 | 84.88 | 11.33 |
| Au | 1.1748 | 11.360 | 84.88 | 11.33 |
| Pt | 1.1748 | 11.360 | 84.88 | 11.33 |

## 4. Conclusion

In this paper, a $Cu_2O/TiO_2$ thin film solar cell has been simulated through Solar Cell Capacitance Simulator (SCAPS-1D) to investigate the influences the defect density and back contact metals. Simulation results show that short circuit current ($J_{SC}$), open circuit voltage ($V_{OC}$), fill factor (FF) and power conversion efficiency (PCE) are deteriorated as the defect densities increase. Moreover, current-voltage characteristics of this cell remarkably improve for Ni, Au and Pt metal back contacts. Although the use of Au and Pt metals as back contacts slightly increases short circuit current ($J_{SC}$), Ni metal is selected as optimised back contact of the proposed device to reduce fabrication cost. The optimised values of $J_{SC,}$ $V_{OC,}$ FF and PCE at operating temperature of 300 K are respectively 11.358 mA/cm$^2$, 1.1748 V, 84.88 % and 11.33 %. These results are in well agreement with the results reported by earlier studies [30, 54, 55]. The highest obtainable efficiencies of metal oxide semiconductor-based heterojunction solar cells are 20% theoretically [16] and 3.83% experimentally [17]. This work may be the important guidelines for researchers to design and fabricate $Cu_2O/TiO_2$ thin film solar cells.

**Acknowledgements**

Authors are thankful to Dr. Marc Burgelman, Honorary Professor, University of Gent, Belgium, for providing SCAPS-1D software.

## Reference

[1] B. Sunden, Hydrogen, Batteries and Fuel Cells, Academic Press, Elsevier, 1-13 (2019).
[2] G. P. Hammond, P. J. G. Pearson, Energy Policy **52**, 1 (2013).
[3] Q. Chao, Y. Wang, Z. Lou, S. Yue, W. Niu, J. Alloy. Compd. **779**, 387 (2019).
[4] Z. Li, K. Tong, R. Shi, Y. Shen, Y. Zhang, Z. Yao, J. Fan, M. Thwaites, G. Shao, J. Alloy. Compd. **695**, 3116 (2017).
[5] L. Lu, M. Guo, S. Thornley, X. Han, J. H. Hu, M. J. Thwaites, G. Shao, Sol. Energ. Mat. Sol. C. **149**, 310 (2016).
[6] Y. Shen, M. Guo, X. Xia, G. Shao, Acta Mater. **85**, 122 (2015).
[7] X. W. Zou, H. Q. Fan, Y. M. Tian, M. G. Zhang, X. Y. Yan, RSC Adv. **5**, 23401 (2015).
[8] R. Jose, T. Velmurugan, R. Seeram, J. Am. Ceram. Soc. **92**, 289 (2009).
[9] E. Fortunato, P. Barquinha, R. Martins, Adv. Mater. **24**, 2945 (2012).
[10] B. Zaidi, M. S. Ullah, B. Hadjoudja, S. Gagui, N. Houaidji, B. Chouial, C. Shekhar, J. Nano-Electron. Phys. **11**, 02030 (2019).
[11] E. Fortunato, D. Ginley, H. Hosono, D. C. Paine, MRS Bull. **32**, 242 (2007).
[12] S. Rühle, A. Y. Anderson, H. N. Barad, B. Kupfer, Y. Bouhadana, E. Rosh-Hodesh, Arie Zaban, J. Phys. Chem. Lett. **3**, 3755 (2012).
[13] H. Bitam, B. Zaidi, B. Hadjoudja, C. Shekhar, S. Gagui, M. S. Ullah, Applied Sollar Energy **58**, 198 (2022).
[14] M. Sibiński, K. Znajdek, Innovative elastic thin-film solar cell structures, Solar Cells – Thin Film Technologies, Intech, 253-274 (2011).
[15] L. Boudaoud, S. Khelifi, M. Mostefaoui, A. K. Rouabhia, N. Sahouane, Energy Procedia **74**, 745 (2015).
[16] L. Zhu, Development of Metal Oxide Solar Cells through Numerical Modelling, PhD Thesis, University of Bolton, 1-204 (2012).
[17] T. Minami, Y. Nishi, T. Miyata, J. I. Nomoto, Appl. Phys. Express **4**, 062301 (2011).
[18] D. Li, C. Chien, S. Deora, P. Chang, E. Moulin, J. Lu, Chem. Phys. Lett. **501**, 446 (2011).
[19] S. Hussain, C. Cao, Z. Usman, Z. Chen, G. Nabi, W. S. Khan, Z. Ali, F. K. Butt, T. Mahmood, Thin Solid Films **522**, 430 (2012).
[20] A. R. Zainun, T. Sakamoto, U. M. Noor, M. Rusop, M. Ichimura, Material Letter **66**, 254 (2012).
[21] M. Ichimura, Y. Kato, Mat. Sci. Semicon. Proc. **16**, 1538 (2013).
[22] B. Zaidi, A. Kerboub, T. Bouarroudj, C. Shekhar, T. Mahmood, M. A. Saeed, J. Optoelectron. Adv. M. **25**(11-12), 549 (2023).
[23] P. Sawicka-Chudy, M. Sibiński, G. Wisz, E. R. Wilusz, M. Cholewa, IOP Conf. Series: Journal of Physics: Conf. Series **1033**, 012002 (2018).
[24] M. Faheem, B. Basha, M. S. Al-Buriahi, Z. A. Alrowaili, K. Mahmood, A. Ali, M. R. Khawar, C. Cho, D. Choi, S. Hussain, Results Phys. **64**, 107896 (2024).
[25] A. S. Mathur, P. P. Singh, S. Upadhyay, N. Yadav, K. S. Singh, D. Singh, B. P. Singh, Sol. Energy **233**, 287 (2022).
[26] A. S. Mathur, B. P. Singh, Optik **212**, 164717 (2020).
[27] A. S. Mathur, S. Dubey, Nidhi, B. P. Singh, Optik **206**, 163245 (2020).
[28] D. Rached, R. Mostefaoui, Thin Solid Films **516**(15), 5087 (2008).
[29] S. Ruhle, H. N. Barad, Y. Bouhadana, D. A. Keller, A. Ginsburg, K. Shimanovich, K. Majhi, R. Lovrincic, A. Y. Andersona, A. Zaban, Phys. Chem. Chem. Phys. **16**, 7066 (2014).
[30] S. S. C. Aydin, J. Optoelectron. Adv. M. **23**(3-4), 157 (2021).
[31] H. Toura, Y. H. Khattak, F. Baig, B. M. Soucase, M. E. Touhami, Sol. Energy **194**, 932 (2019).
[32] V. T. Babu, N. Nair, K. S. Parvathy, B. S. Panicker, D. Ardra, S. Gpika, M. Anjitha, S. K. Ram, Materials Today: Proceedings **65**(1), 408 (2022).
[33] M. R. Johan, M. S. M. Suan, N. L. Hawari, H. A. Ching, Int. J. Electrochem. Sci. **6**, 6094 (2011).
[34] N. Serin, T. Serin, S. Horzum, Y. Celik, Semicond. Sci. Technol. **20**, 398 (2005).
[35] G. Amin, ZnO and CuO nanostructures: low temperature growth, characterization, their optoelectronic and sensing applications, 1st ed. LiU-Tryck: Norrköping, Sweden, SE-601 74, 1-80 (2012)
[36] M. I. Hossain, F. H. Alharbi, N. Tabet, Sol. Energy **120**, 370 (2015).
[37] Y. Abdu, A. O. Musa, Journal of Pure and Applied Sciences **2**(2), 8 (2009).
[38] P. Sawicka-Chudy, G. Wisz, S. Górny, Ł. Głowa, M. Sibiński, M. Cholewa, J. Nanoelectron. Optoe. **13**(5), 715 (2018).
[39] S. S. Jeong, A. Mittiga, E. Salza, A. Masci, S. Passerini, Electrochim. Acta **53**, 2226 (2008).
[40] B. S. Li, K. Akimoto, A. Shen, J. Cryst. Growth **311**, 1102 (2009).
[41] Y. S. Lee, J. Heo, M. T. Winkler, S. C. Siah, S. B. Kim, R. G. Gordon, T. Buonassisi, J. Mater. Chem. A **1**, 15416 (2013).
[42] M. I. Hossain, F. H Alharbi, Materials Technology: Advanced Performance Materials **28**, 88 (2013).
[43] R. Rivera, A. Stashans, Defects in $TiO_2$ Crystals, Proceedings of the International Multi Conference of Engineers and Computer Scientists (IMECS), Hong Kong, Vol. **II** (2013).
[44] I. Kars, S. S. Cetin, B. Kinac, B. Sarikavak, A. Bengi, H. Altuntas, M. K. Ozturk, S. Ozcelik, Surface and Interface Analysis **42**, 1247 (2010).

[45] A. Andersson, N. Johansson, P. Bröms, N. Yu, D. Lupo, W. R. Salaneck, Advanced Materials **10**(11), 859 (1998).
[46] A. Froitzheim, R. Stangl, M. Kriegel, L. Elstner, W. Fuhs, Proceedings of the 3rd Worldconference on Photovoltaic Solar Energy Conversion, Osaka, Japan **1**, 279 (2003).
[47] H. Zhu, A. K. Kalkan, J. Hou, S. J. Fonash, AIP Conf. Proc. **462**, 309 (1999).
[48] F. Smole, J. Krč, J. Furlan, Sol. Energ. Mat. Sol. C **34**, 385 (1994).
[49] M. Burgelman, P. Nollet, S. Degrave, Thin Solid Films **361**, 527 (2000).
[50] K. Decock, S. Khelifi, M. Burgelman, Thin Solid Films **519**, 7481 (2011).
[51] K. Decock, P. Zabierowski, M. Burgelman, J. Appl. Phys. **111**, 043703 (2012).
[52] M. Burgelman, K. Decock, A. Niemegeers, J. Verschraegen, S. Degrave, SCAPS Manual, ELIS-University of Gent, 2021.
[53] A. Kumar, A. D. Thakur, Jpn. J. Appl. Phys. **57**, 08RC05, 1 (2018).
[54] M. Mostefaoui, H. Mazari, S. Khelifi, A. Bouraiou, R. Dabou, Energy Procedia **74**, 736 (2015).
[55] K. Tan, P. Lin, G. Wang, Y. Liu, Z. Xu, Y. Lin, Solid-State Electronics **126**, 75 (2016).

*Corresponding author: kumarashimbiswas@gmail.com